

REPORT DOCUMENTATION PAGE

Form Approved
OMB No. 0704-0188

Public reporting burden for this collection of information is estimated to average 1 hour per response, including the time for reviewing instructions, searching existing data sources, gathering and maintaining the data needed, and completing and reviewing this collection of information. Send comments regarding this burden estimate or any other aspect of this collection of information, including suggestions for reducing this burden to Department of Defense, Washington Headquarters Services, Directorate for Information Operations and Reports (0704-0188), 1215 Jefferson Davis Highway, Suite 1204, Arlington, VA 22202-4302. Respondents should be aware that notwithstanding any other provision of law, no person shall be subject to any penalty for failing to comply with a collection of information if it does not display a currently valid OMB control number. **PLEASE DO NOT RETURN YOUR FORM TO THE ABOVE ADDRESS.**

1. REPORT DATE (DD-MM-YYYY) 30-06-2003		2. REPORT TYPE Technical Paper		3. DATES COVERED (From - To)	
4. TITLE AND SUBTITLE Development of GOX/Kerosene Swirl-Coaxial Injector Technology				5a. CONTRACT NUMBER F04611-01-C-0010	
				5b. GRANT NUMBER	
				5c. PROGRAM ELEMENT NUMBER	
6. AUTHOR(S) Gary C. Cheng (Univ. of AL); Rory R. Davis (Convergence Engineering); Curtis W. Johnson, Jeffrey A. Muss, Daniel A. Greisen (Sierra Engineering); Richard K. Cohn (AFRL/PRSA)				5d. PROJECT NUMBER BMDO	
				5e. TASK NUMBER SBRU	
				5f. WORK UNIT NUMBER	
7. PERFORMING ORGANIZATION NAME(S) AND ADDRESS(ES) Sierra Engineering Inc. Carson City NV				8. PERFORMING ORGANIZATION REPORT NUMBER	
9. SPONSORING / MONITORING AGENCY NAME(S) AND ADDRESS(ES) Air Force Research Laboratory (AFMC) AFRL/PRS 5 Pollux Drive Edwards AFB CA 93524-7048				10. SPONSOR/MONITOR'S ACRONYM(S)	
				11. SPONSOR/MONITOR'S NUMBER(S) AFRL-PR-ED-TP-2003-181	
12. DISTRIBUTION / AVAILABILITY STATEMENT Approved for public release; distribution unlimited.					
13. SUPPLEMENTARY NOTES For presentation at the AIAA Joint Propulsion Conference in Huntsville, AL, taking place 20-23 July 2003.					
14. ABSTRACT					
20030812 208					
15. SUBJECT TERMS					
16. SECURITY CLASSIFICATION OF:			17. LIMITATION OF ABSTRACT	18. NUMBER OF PAGES	19a. NAME OF RESPONSIBLE PERSON
a. REPORT Unclassified	b. ABSTRACT Unclassified	c. THIS PAGE Unclassified	A	9	Leilani Richardson
					19b. TELEPHONE NUMBER (include area code) (661) 275-5015



AIAA 2003-4751

**Development of GOX/Kerosene Swirl-
Coaxial Injector Technology**

Gary C. Cheng
University of Alabama Birmingham
Birmingham, AL

Rory R. Davis
Convergence Engineering Corporation
Gardnerville, NV

Curtis W. Johnson, Jeffrey A. Muss, and Daniel A. Greisen
Sierra Engineering Inc.
Carson City, NV

Richard K. Cohn
Air Force Research Laboratory
Edwards Air Force Base, CA

**39th AIAA/ASME/SAE/ASEE Joint Propulsion
Conference and Exhibit**

20-24 July 2003

Huntsville Alabama

For permission to copy or to republish, contact the copyright owner named on the first page. For
AIAA-held copyright, write to AIAA Permissions Department,
1801 Alexander Bell Drive, Suite 500, Reston, VA 20191-4344

Development of GOX/Kerosene Swirl-Coaxial Injector Technology

Gary C. Cheng*

University of Alabama Birmingham
Birmingham, AL

Rory R. Davis

Convergence Engineering Corp.

Curtis W. Johnson[#], Jeffrey A. Muss*, and Daniel A. Greisen

Sierra Engineering Inc.
Carson City, NV

Richard K. Cohn[#]

Air Force Research Laboratory
Edwards AFB, CA

ABSTRACT

In developing an advanced liquid rocket engine, injector design is critical to obtaining the dual goals of long engine life and high-energy release efficiency in the main combustion chamber. A joint effort of Sierra Engineering (Sierra) and the Propulsion Directorate of the Air Force Research Lab (AFRL) was conducted to develop a design methodology, utilizing both high-pressure cold-flow testing and uni-element hot fire testing, to create a high performing, swirl coaxial injector for multi-element combustor use. The results of this joint effort have been documented in a series of JANNAF and AIAA meeting papers¹⁻⁴. The present work studies the hot flow environment specifically the multiple element swirl coaxial injector. Numerical simulations were performed with a multiple-phase, pressure-based computational fluid dynamics (CFD) code, FDNS⁵⁻⁸. CFD results produced loading environments for an ANSYS finite element thermal/structural model. Since the fuels are injected at a temperature below its critical temperature, the effect of phase change and chemical reactions needs to be accounted for in the CFD model. A homogeneous spray approach with a real-fluid property model⁵⁻⁷ was employed in the FDNS code to simulate the spray combustion phenomena over a wide range of operating conditions. Future work, which will not be presented in this paper, will compare these numerical results to planned hot fire test results.

Proper injector design is critical to achieving long engine life while providing high combustion efficiency in rocket combustion chambers. Gas-centered swirl coaxial injectors, which swirl liquid fuel around a gaseous oxygen core, show promise for the next generation hydrocarbon fueled staged-combustion rocket engines. Introducing a swirl component in the injector flow can enhance the propellant mixing and thus improve engine performance. These injectors can be designed with large element thrusts, reducing manufacturing costs, while providing good spatial uniformity and a low face temperature, both of which improve engine life.

Sierra Engineering and the Air Force Research Laboratory (AFRL) have undertaken a program to develop design guidelines for gas-centered swirl coaxial injectors. The element will initially be used in an Alternate Fuels Testbed (AFT) combustor to test hydrocarbon fuel performance and operability. In order to produce meaningful results, the 2000 lb_f thrust multi-element AFT combustor has to be high performing and adaptable to different hydrocarbon based fuels. The combustor operates on ambient temperature gaseous oxygen and an array of fuels. The combustor is designed with removable injector elements, allowing the element geometry to be tailored for each fuel if it proves necessary.

A major issue with designing hardware, particularly long life hardware, is determining the environments in which the hardware will be required to survive. In the case of the AFT combustor one such problem was accurate estimation of heat loading on the injector

INTRODUCTION

[#]Member AIAA

^{*}Senior Member AIAA

Copyright © 2003 by Sierra Engineering Inc. Published by American Institute of Aeronautics and Astronautics, Inc. with permission Distribution A(pending): Approved for Public Release; Distribution is unlimited. Release # AFRL-ERS-PAS 03-????

experimental results can be found in references 2 and 4. The final series simulated hot fire operation of the 5-element AFT combustor with RP-1 and gaseous oxygen as propellants. The numerical simulation of hot fire uni-element injector flows focused on the validation of the spray combustion model without the inter-element effect, whereas the simulation of the AFT combustor took the inter-element effect into account. Previous papers² reported in detail on the CFD solutions completed, while this paper presents only the multi-element CFD solutions and their use for injector face thermal/structural analysis.

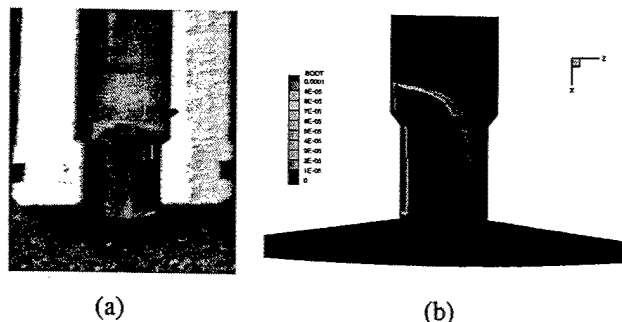


Figure 2: (a) cut-away view of injector 11 showing soot formation on injector. (b) Soot formation from CFD results.

The hot fire simulations with gaseous O_2 as the oxidizer and RP-1 as the fuel were performed for the 5-element AFT engine operating pressures of 1000 and 2000 psia. A converging injector element was used in these simulations. As a result of the non-axisymmetric nature of the injection element, a 72° pie section of the engine, encompassing a complete element, was modeled (Figure 3). The operating condition, boundary conditions, and simulated engine geometry are depicted in Figure 4. Although the AFT engine includes a sonic throat, the simulation considers only the chamber barrel portion of the test article, with the downstream mass conservation boundary condition imposed.

Computer hardware limitations resulted in a grid system that was not sufficient to resolve the steep gradients at the reaction front, but the location of the reaction zone is readily identified.

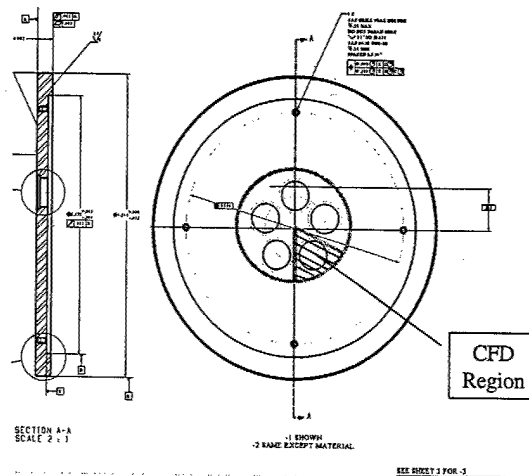


Figure 3. Depiction of Injector Face Computational Boundary

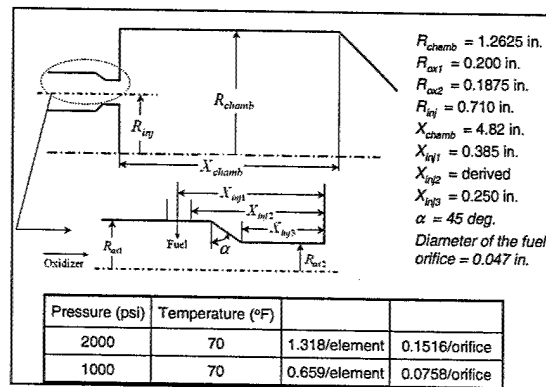


Figure 4. Flow and Boundary Conditions

Temperature and velocity fields from the chamber centerline to the outer wall across the center of an injection element are shown for both cases in Figure 5 and Figure 8. Significant reaction occurs within the injection element for the 1000 psi case (Figure 5 and Figure 6), and the main chamber flow contains two large recirculations - a strong rollup along the centerline where the adjacent elements interact and a long "backflow" along the chamber wall. In contrast, the reaction is stabilized downstream of the element exit for the 2000 psi case (Figure 8). This is due to higher liquid injection velocity, and thus shorter residence time of RP-1 in the injector element. The cold oxidizer lasts longer in the combustion chamber for the high-pressure case, with small recirculations visible at the injector face-wall intersection and in the near-face region between the elements. The reason for the low-pressure case to have stronger recirculations is the hotter mixture flow (and thus higher flow speed) exit from the injector and expansion in the chamber.

In addition, the high-pressure case demonstrates slower mixing and less uniformity due to higher mass flux through the stream tube. This is because with the same O/F ratio and injection gas speed for both operating conditions, the high-pressure case has high mass flow rate for both liquid RP-1 and GOX through the injector of the same diameter. Close-up views of the injector outlet temperature (Figure 6 and Figure 9), the cross-sectional temperature distributions (Figure 7 and Figure 10), and the streamlines of injector flows (Figure 11 and Figure 14) reinforce these observations.

Radial temperature (Figure 12 and Figure 15) and oxidizer-to-fuel mass mixture ratio (MR) (Figure 13 and Figure 16) are presented for both operating conditions. Both sets of profiles are much more uniform, both axially and radially for the low pressure (1000 psi) operating condition. This is consistent with the temperature/velocity contours presented in Figure 5-9. It is apparent that the oxidizer core persists much further into the chamber for the high P_c case.

Temperature Contours & Velocity Vectors at the Symmetry Plane of an Injector (1000 psi)

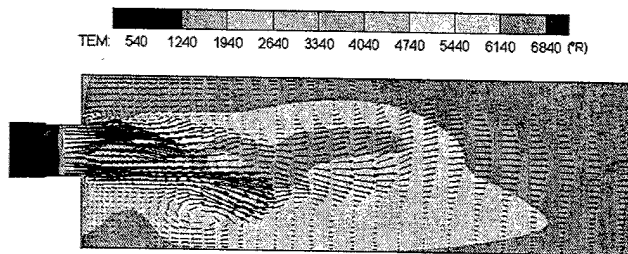


Figure 5. Predicted Combustion Chamber Gas Temperature Contours and Velocity Vectors for AFT Operation at $P_c=1000$ psi

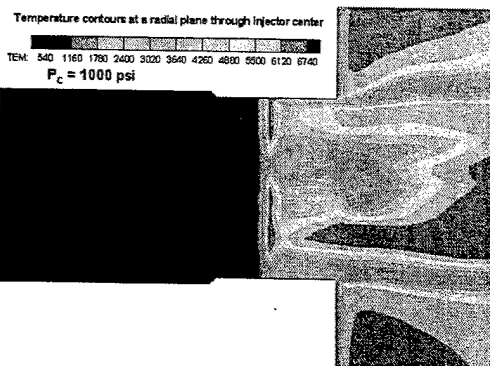


Figure 6. Near-Face Combustion Chamber Gas Temperature Distribution for AFT Operation at $P_c=1000$ psi

Temperature Contours of AFT Multi-Injector Engine ($P_c = 1000$ psi)

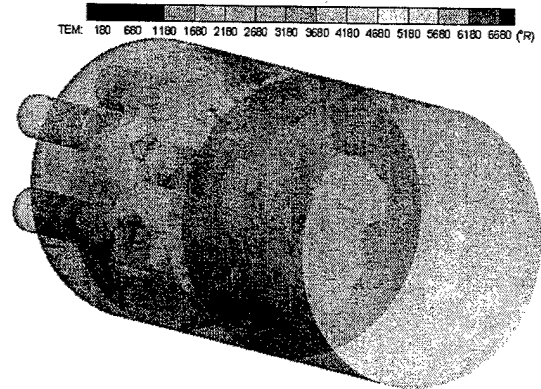


Figure 7. Gas Temperature Distributions of Different Cross Sections for AFT Operation at $P_c=1000$ psi

Temperature Contours & Velocity Vectors at the Symmetry Plane of an Injector (2000 psi)

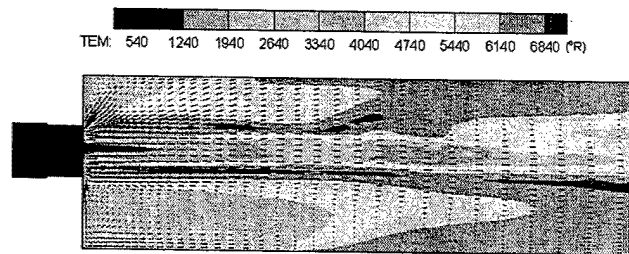


Figure 8. Predicted Combustion Chamber Gas Temperature Contours and Velocity Vectors for AFT Operation at $P_c=2000$ psi

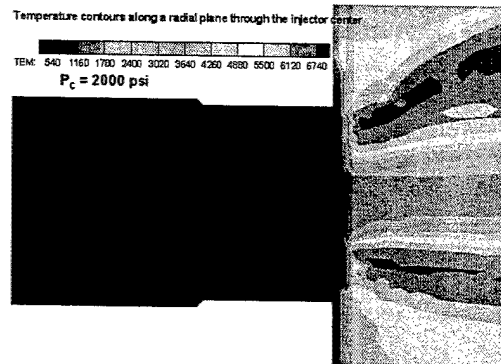


Figure 9. Near-Face Gas Temperature Distribution for AFT Operation at $P_c=2000$ psi

Temperature Contours of AFT Multi-Injector Engine ($P_c = 2000$ psi)

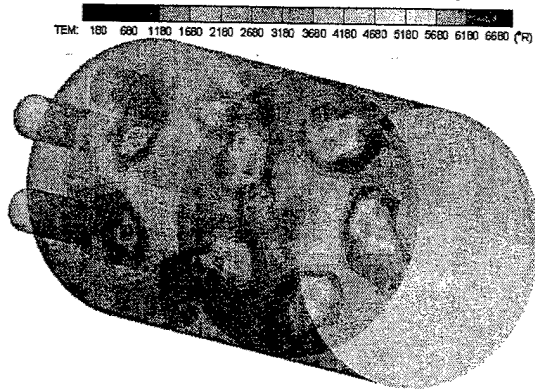


Figure 10. Gas Temperature Distributions of Different Cross Sections for AFT Operation at $P_c=2000$ psi

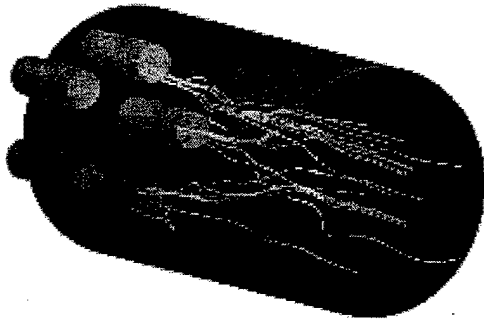


Figure 11. Streamlines (Colored with Temperatures) of Injector Flow for AFT Operation at $P_c=1000$ psi

Radial O/F Ratio Profiles at Various Axial Locations from Face Plate

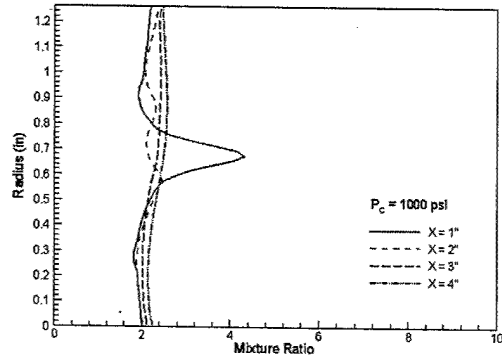


Figure 13. Radial O/F Mixture Ratio Profiles for AFT Operation at $P_c=1000$ psi

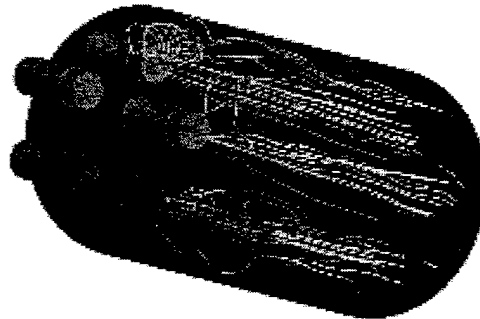


Figure 14. Streamlines (Colored with Temperatures) of Injector Flow for AFT Operation at $P_c=1000$ psi

Radial Temperature Profiles at Various Axial Locations from Face Plate

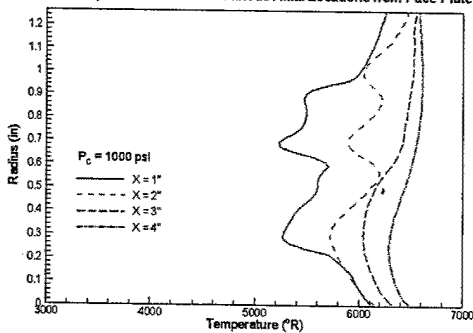


Figure 12. Radial Gas Temperature Profiles for AFT Operation at $P_c=1000$ psi

Radial Temperature Profiles at Various Axial Locations from Face Plate

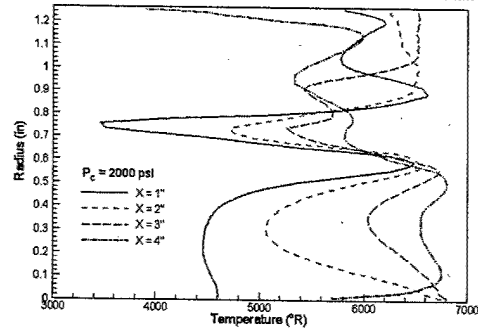


Figure 15. Radial Gas Temperature Profiles for AFT Operation at $P_c=2000$ psi

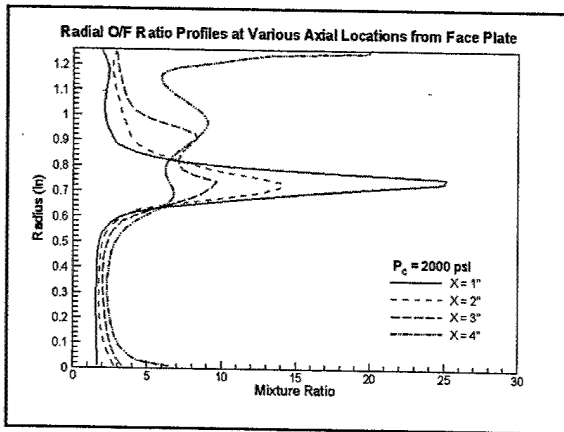


Figure 16. Radial O/F Mixture Ratio Profiles for AFT Operation at $P_c=2000$ psi

DISCUSSIONS

Effects of Chamber Pressure

The effect of chamber pressure (P_c) on mixing efficiency was examined for the multi-element AFT configurations. Cold flow simulation and testing, indicate that chamber pressure does not have a strong effect on the liquid propellant distribution, and thus the mixing efficiency². Therefore, this injector element should perform well under throttled conditions. This has been demonstrated in references 1, 3, and 5 where this converging element demonstrated C^* efficiencies in excess of 95% for a wide range of pressure conditions and for a variety of fuels. The multi-element hot fire simulations show that the combustion characteristics change dramatically with P_c . This change is in part due to the flame front being pushed out of the element as the oxidizer mass flux increases. This confirmed our finding from previous studies⁷⁻⁸ that the mixing characteristic of hot flow is quite different from its cold flow counterpart. This is because the combustion in the shear layer between the oxidizer and fuel inhibits the propellants from further mixing. The flame position affects the velocity magnitude of the mixture exit from the injector element, and thus influences the location and strength of near-face recirculations. The AFT injectors were designed for a 1000 psia chamber pressure, where the 1000 psia simulation was assumed to best represent the flowfield expected during engine operation.

Determination of Face Heat Flux

The CFD predicted injector face near wall velocities, mixture ratio, and temperature were reviewed with the objective of deriving representative injector face heat transfer characteristics. The prediction region, see Figure 3, was broken down into three areas, the area with a radius smaller than the element internal radius, the inter-element area (i.e. element internal radius to element outer radius), and the area with a radius larger than the element. The predictions of each area were evaluated for maximums, minimums, and variation of the predicted parameter.

Table 1 presents the estimated injector face heat transfer characteristics. The injector face heat transfer characteristics vary considerably between the three areas, with the presented data representing a conservative estimate within each area.

The injector face heat transfer conditions estimated prior to the completion of the CFD analyses were 2649°R and 0.0024 Btu/in²-sec-°F.

Table 1. Injector Face Heat Transfer Characteristics

Area	Recovery Temp (°R)	Heat Transfer Coefficient (Btu/in ² -sec-°F)
Inside of Elements	5077	0.000713
Inter-Elements	3160	0.00045
Outside of Elements	4457	0.00021

Stress Analysis

The stress analyses were completed using the ANSYS finite element structural analysis program. The hardware was designed to run at relatively high pressures and no barrier cooling in the GOX hydrocarbon combustor. Consequently run times were required to be short (0.7 seconds at 100% power) due to throat heat loading.

Figure 16 shows a cross section of the injector assembly. The injector consists of 5 swirl coaxial elements in a single row. Each element is sandwiched in between the injector face and the GOX manifold. Material trades were performed for the injector element ox post and faceplate. A preferred combination was determined to be a Nickel 200 ox post, and a half-hard OFHC Copper or a half-hard Cartridge Brass face.

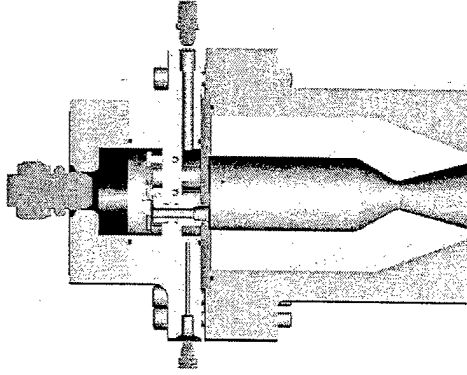


Figure 17. Cross Section of the Injector Assembly

A pie slice finite element model of the chamber was developed, including ox post fit within the face plate and preload bolts. Transient heat transfer analysis was performed, and the resulting temperatures were fed into a quasi-static thermal/pressure stress analysis. The stress analysis used elastic temperature-dependent material properties.

Heat transfer loads were determined from the steady state CFD as discussed above. Reasonable pre-chill, firing, and shutdown transients were defined for thermal and pressure loading purposes as well. The model was run with an OFHC Copper faceplate.

Figure 18 shows the transient thermal response in the injector area. In this short period, face temperatures are quite benign, as compared to the original prediction.

Figure 19 shows the maximum temperature distribution at the end of 0.70 sec of firing. Note for this duration that injector hot face temperature is adequately low and the cool side temperature is well below fuel coking limits for copper.

Figure 20 shows the von Mises stress response of the parts at the end of 0.70 sec firing. Yellow and "hotter" areas indicate significant plasticity, which occurs at the ox post hot face and its interface with the face plate. This analysis used zero radial clearance of the ox post within the face plate, giving maximum stress when the face gets hot and the parts compress together radially at the face.

Note that due to the closure of the inter-part radial gap, ox post end seals are optional. Any small amount of initial fuel leakage would actually enhance face cooling as a transpiration effect.

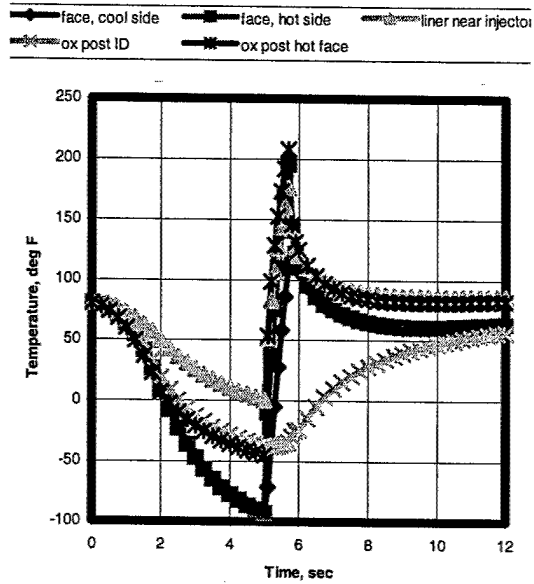


Figure 18. Transient Temperature Response for 0.70 sec Firing Starting at 5.0 sec

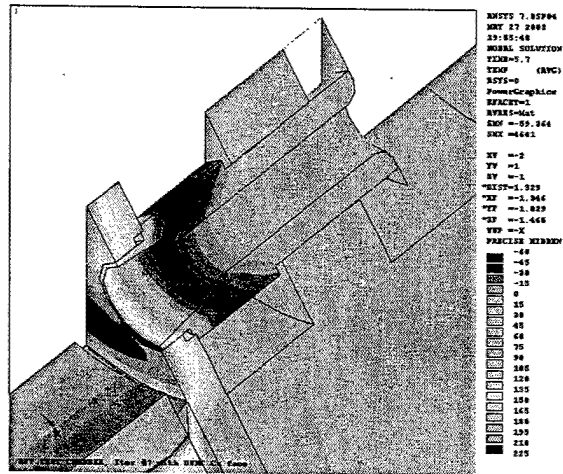


Figure 19. Temperature Response at End of 0.70 sec Firing (deg F Contours)

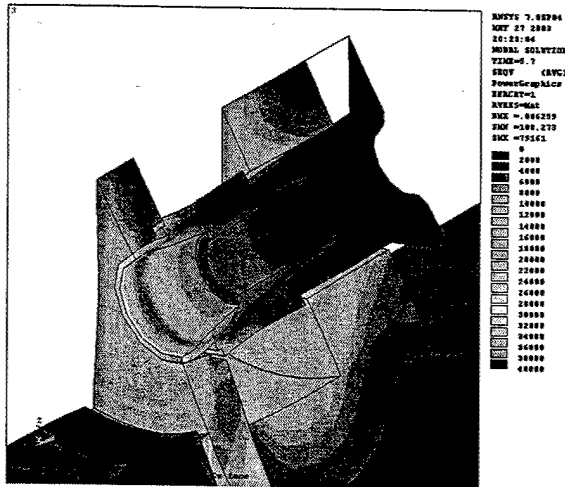


Figure 20. von Mises Stress Response at End of 0.70 sec Firing (Deflections Exaggerated)

CONCLUSIONS

The model identifies the physical phenomena producing the mixing in these elements. The elements swirl the fuel around the inside of the GOX post. That fuel is swept out of the GOX post in a sheet and then entrained into the high velocity GOX flow downstream of the element. However, sufficient simulations have not been completed to determine the sensitivity of the mixing to major design parameters, such as GOX velocity, fuel swirl, and injector geometry. The simulations completed suggest that the models are capable of providing meaningful results for these types of parametric studies.

Proper design allows a fuel film layer to exist as the propellants exit the injector. This layer can lower temperatures at the injector face and allow the injector face to operate in a reduced heat flux environment. Thermal/structural analyses suggest the resulting injector can be designed to meet current combustor requirements out of commonly available materials.

ACKNOWLEDGEMENTS

This work was performed as part of a BMDO Phase II SBIR (F04611-C-00-0010) administered by AFRL/West, Edwards AFB, CA 93524. Funding for AFT hardware design, fabrication and testing provided by AFRL/PRSE (Edwards AFB). Uni-element cold flow and hot fire test support provided by AFRL/PRSA (Edwards AFB).

REFERENCES

1. Cohn, R.K., Strakey, P.A., Bates, R.W., Talley, D.G., Muss, J.A. and Johnson, C.W.; "Swirl Coaxial Injector Development", AIAA-2003-0124, 2003.
2. Muss, J.A., Johnson, C.W., Cheng, G.C., and Cohn, R.K., "Numerical Cold Flow and Combustion Characterization of Swirl Coaxial Injectors," AIAA-2003-0125, 2003.
3. Muss, J.A., Johnson, C.W., Cohn, R.K., Strakey, P.A., Bates, R.W. and Talley, D.G., "Swirl Coaxial Injector Development Part I – Test And Results", 38th JANNAF Combustion Subcommittee Meetings, Destin, FL, April 8-12, 2002.
4. Cheng, G.C., Johnson, C.W., Muss, J.A., and Cohn, R.K., "Swirl Coaxial Injector Development, Part II: CFD Modeling," 2002 JANNAF CS/APS/PSHS/MSS Joint Meeting, Destin, FL, April 2002.
5. Cohn, R.K., Danczyk, S.A., and Bates, R.W. "A Comparison of the Performance of Hydrocarbon Fuels in a Uni-Element Combustor," AIAA Paper 2003-4752.
6. Cheng, G.C. and Farmer, R.C., "CFD Spray Combustion Model for Liquid Rocket Engine Injector Analyses," AIAA Paper 2002-0785.
7. Cheng, G.C., Anderson, P.G., and Farmer, R.C., "Development of CFD Model for Simulating Gas/Liquid Injectors in Rocket Engine Design," AIAA Paper 97-3228, 1997.
8. Farmer, R.C., Cheng, G.C., Trinh, H., and Tucker, K., "A design Tool for Liquid Rocket Engine Injectors," AIAA 2000-3499, 2000.
9. Chen, Y.S., "Compressible and Incompressible Flow Computations with a Pressure Based Method," AIAA Paper 89-0286, 1989.
10. Hirschfelder, J.O., et al, "Generalized Equations of State for Gases and Liquids," *IEC*, 50, pp.375-385, 1958.
11. Hirschfelder, J.O., et al, "Generalized Excess Functions for Gases and Liquids," *IEC*, 50, pp.386-390, 1958.
12. Reid, R.C., et al, The Properties of Gases & Liquids, 4th ed., McGraw-Hill, 1987.
13. Gordon, S., and B.J. McBride, "Computer Program for Calculation of Complex Chemical Equilibrium Compositions, Rocket Performance, Incident and Reflected Shocks, and Chapman-Jouget Detonations," NASA-SP-273, 1971.
14. Saad, Y., and Schultz, M.H., SIAM Journal of Sci. Stat. Comput., Vol. 7, pp. 856-869, 1986.

15. Muss, J.A.; The Measurement of Mixture Fraction and Scalar Dissipation Rate in Turbulent Jet

Flames, Doctoral Dissertation, UC Berkeley, 1997